Steel and Composite Structures, *Vol. 31, No. 4 (2019) 373-385*
DOI: https://doi.org/10.12989/scs.2019.31.4.373

In-plane structural analysis of blind-bolted composite frames with semi-rigid joints

Rumman Waqas [*1], Brian Uy [2a], Jia Wang [2b] and Huu-Tai Thai [3c]

[1] *School of Civil and Environmental Engineering, The University of New South Wales, Sydney, NSW 2052, Australia*
[2] *School of Civil Engineering, The University of Sydney, Sydney, NSW 2006, Australia*
[3] *Department of Infrastructure Engineering, The University of Melbourne, Parkville, VIC 3010, Australia*

(*Received November 29, 2018, Revised March 28, 2019, Accepted March 31, 2019*)

Abstract. This paper presents a useful in-plane structural analysis of low-rise blind-bolted composite frames with semi-rigid joints. Analytical models were used to predict the moment-rotation relationship of the composite beam-to-column flush endplate joints that produced accurate and reliable results. The comparisons of the analytical model with test results in terms of the moment-rotation response verified the robustness and reliability of the model. Abaqus software was adopted to conduct frame analysis considering the material and geometrical non-linearities. The flexural behaviour of the composite frames was studied by applying the lateral loads incorporating wind and earthquake actions according to the Australian standards. A wide variety of frames with a varied number of bays and storeys was analysed to determine the bending moment envelopes under different load combinations. The design models were finalized that met the strength and serviceability limit state criteria. The results from the frame analysis suggest that among lateral loads, wind loads are more critical in Australia as compared to the earthquake loads. However, gravity loads alone govern the design as maximum sagging and hogging moments in the frames are produced as a result of the load combination with dead and live loads alone. This study provides a preliminary analysis and general understanding of the behaviour of low rise, semi-continuous frames subjected to lateral load characteristics of wind and earthquake conditions in Australia that can be applied in engineering practice.

Keywords: composite frames; beam-to-column joints; initial stiffness; moment capacity; moment-rotation relationship; lateral loads; frame analysis; semi-rigid connection

1. Introduction

Concrete-filled steel tubular (CFST) columns have achieved widespread popularity in engineering practice due to their exceptional static and earthquake resistant properties that include high stiffness, strength, energy absorption capacity and ductility (Han *et al*. 2008). The concrete infill in CFST columns provides a higher bearing capacity as the concrete prevents local buckling of the steel tube and the steel tube provides confinement to the concrete and prevents it from spalling.

During the last two decades, numerous studies have been attempted to explore the behaviour of composite joints with CFST columns such as Nogueiro *et al*. (2009), Ma *et al*. (2011), Uy (2012), Han *et al*. (2016), Uy *et al*. (2017), Beena *et al*. (2017) and Li *et al*. (2017). The experimental and analytical results demonstrate that the composite joints exhibit higher stiffness and improved performance as compared to the traditional steel or concrete joints.

The development of blind bolts has helped to get rid of the extensive welding procedure that not only requires high tolerance but also is expensive and time consuming. These bolts require installation from one side only and help to reduce the amount of work required on site. Hence, it is an efficient, easy and quick medium to achieve connections with CFST columns.

In conventional analysis of frames, the behaviour of beam-to-column joints is considered as either rigid or pinned. However, in reality most connections used are semi-rigid in nature and experience moment capacities and rotational stiffnesses in the middle of the two extremes specified in EN 1993-1-8 (2010) and EN 1994-1-1 (2004). Therefore, these simplified assumptions may be inaccurate and lead to the wrong interpretation of the structural behaviour of the framing components. The modern design codes such as EN 1993-1-8 and AISC-LRFD (1994) have formally recognized and accepted the consideration of semi-rigid behaviour in joints in order to reflect the actual situation (Thai *et al.* 2016). Hence, the need arises to determine the key properties of the connection to be included in the frame analysis and design.

The behaviour of a joint is represented by its moment-rotation behaviour that depends on three key properties which are initial rotational stiffness, moment resistance and rotational capacity. These properties can be predicted using EN 1993-1-8 (for bare steel joint) and EN 1994-1-1 (for composite joint). However, characteristics of various

∗Corresponding author, Ph.D. Student,
E-mail: r.waqas@student.unsw.edu.au
[a] Professor., E-mail: brian.uy@sydney.edu.au
[b] Ph.D., E-mail: jia.wang@sydney.edu.au
[c] Ph.D., E-mail: tai.thai@unimelb.edu.au

http://www.techno-press.org/?journal=scs&subpage=6 ISSN: 1229-9367 (Print), 1598-6233 (Online)

components involved make it difficult to predict the structural performance reasonably well. Therefore, it requires re-planning of the structure on the basis of sub-model as well as global frame analysis.

Considerable progress has been made in recent years in order to develop an efficient and reliable analytical method to calculate the moment capacity and rotational stiffness of composite connections. Many models have been presented and mostly comprise of the parameters depending on the stiffness, strength or ductility for a given connection and shape parameters treated as a curve fitting parameter (Lee and Moon 2002). Therefore, the expressions prove to be accurate only for the particular type and limited range of data used in the regression analysis. Xiao *et al*. (1996) developed a comprehensive mathematical model to predict the behaviour of various types of endplate connections. The model was validated against test results and parametric studies were performed on a variety of parameters to assess the performance of the connection. Ahmed and Nethercot (1997) proposed a method to predict the initial stiffness and rotational capacity of major axis flush endplate composite connection. Comparison against test results demonstrated that the proposed method was capable of predicting the initial stiffness and rotational capacity with reasonable accuracy. Loh *et al*. (2006b) developed an analytical model to predict the behaviour of semi-rigid flush endplate joints under hogging moment which included the effects of partial shear connection. The comparison between analytical results and test results demonstrated a close agreement in terms of structural performance.

Moreover, Abolmaali *et al*. (2005) used Ramberg-Osgood and Three Parameter Power model to develop equations to predict the moment-rotation (M-Ø) behaviour of flush endplate connections with one row of bolts between tension and compression flanges. The comparison of finite element models with test results demonstrated a good agreement. Thai and Uy (2016) extended the application of the design rules mentioned in EN 1994-1-1 to determine the mechanical properties of a blind bolted flush endplate composite joint with the CFST column. The resistance and stiffness of a new component named 'column face in bending' was calculated using the Gomes *et al*. (1996) model. The analytical model developed was validated against the experimental results by Loh *et al*. (2006a). The empirical equations resulted in accurate and reliable predictions of the test results. This model will also be used in the present study to calculate the stiffness of various components of the blind bolted flush endplate composite joint. Wang *et al*. (2018a) explored the behaviour of demountable composite beam-to-column joints using semi-rigid connections. The authors presented a new approach for the development of moment-rotation relationship of the joint that was verified with the test results from another study by Wang *et al*. (2018b). The proposed model was able to predict the moment-rotation relationship accurately. The prediction was then applied to the frame analysis and the performance of demountable composite frames under gravity and lateral loads was explored.

Extensive research has been carried out to investigate the structural performance of composite frames with semi-rigid connections such as Xiao *et al*. (1996), Liew *et al*. (2000), Hensman and Nethercot (2001), Zhao (2016) and Wang *et al*. (2018b). However, the moment-rotation relationship of these innovative joints still appears to be limited. Little research has focused to investigate the performance of this type of construction in a frame environment, particularly when it comes to theoretical investigation by an accurate and reliable analytical model. Design engineers avoid detailed modelling of composite joints in frames due to complicated geometrical modelling, deficient guidelines, high computational cost and complex interaction behaviour between joints and other structural components (Jeyarajan and Liew 2016). The perceived complexity and accuracy of the existing techniques highlights that there is a considerable scope for improvement in this area. Consequently, a lack of reliable information on the moment-rotation characteristics of the connection is a hurdle in the widespread application of blind bolted composite frames in engineering practice.

Therefore, this study aims to investigate the behaviour of semi-rigid blind bolted composite frames under gravity as well as critical loads of wind or moderate earthquake loading conditions in Australia. The analytical model developed by Thai and Uy (2016) was used for the prediction of initial stiffness, whereas the moment capacity was calculated following the guidelines from EN 1993-1-8 (2010) and EN 1994-1-1 (2004). The predicted moment-rotation model was then used to investigate the flexural behaviour of the composite blind bolted frame under strength and serviceability limit state requirements. The results from this study are expected to be helpful in understanding the complicated behaviour of these frames particularly under lateral loading and also for the design of similar composite frames in engineering practice.

2. Description of the blind bolted flush endplate composite frame

The composite joint under consideration was a flush endplate joint designed under hogging moment and full shear connection in accordance with EN 1994-1-1 (2004). The details of the composite joint are presented in Fig. 1. Four 610UB101 steel beams were connected to a 300 × 300 mm square hollow section column in a cruciform arrangement that represents the internal region of a composite frame. 12 mm thick equal angle sections were welded to the sides of CFST column with the help of the innovative one-side blind bolts. The addition of equal angles between flush endplates and CFST column made it unique as compared with the typical beam-to-column connections. This is equivalent to an increase in the thickness of the CFST column which enhances the initial stiffness to some extent as discussed in a previous study by Waqas *et al*. (2019). Four 12mm thick flush endplates were welded to the steel beams and connected to the steel tubular columns with the help of M20 blind bolts. A 3868 mm × 1600 mm × 120 mm reinforced concrete slab was placed on the top of the steel beam, supported by 1 mm thick profiled steel sheeting which was transversely arranged and welded using 16 shear connectors. The main reinforcements consisted of 8 N12 steel bars uniformly spaced in a single layer for the reinforcement of slab.

3. Development of moment-rotation model

3.1 Prediction of initial stiffness

An accurate analysis of the frame depends on the correct prediction of the initial stiffness of the connection. A combination of the analytical model developed by Thai and Uy (2016) and the guidelines specified in EN 1993-1-8 (2010) was used to calculate the stiffness coefficients of various components of the connection which identified in Fig. 2. Fig. 3 presents the stiffness model for the flush endplate joint developed by Thai and Uy (2016) that has two rows of bolt in tension and was used in this study for calculating the initial stiffness of the composite joint.

For a composite joint, the rotational stiffness should be calculated based on the flexibility of its basic joint components as expressed in Eq. (1). Each of these components is denoted by an elastic stiffness coefficient k_i, as stated in EN 1993-1-8 (2010). The specific stiffness of each joint components is highlighted in Fig. 2 as k_1, k_2, k_3, k_4, k_5, k_{10}, $k_{s,r}$, $k_{sc/Es}$ and can be calculated using the following mathematical equations

$$S_{ini} = \frac{Ez_{eq}^2}{\frac{1}{k_1} + \frac{1}{k_2} + \frac{1}{k_{eq}}} \tag{1}$$

where E is the Young's modulus of steel, keq is the equivalent stiffness coefficient and zeq is the lever arm. k1 and k2 are infinite due to the presence of infill concrete. Therefore, Eq. (1) can be simplified as follows

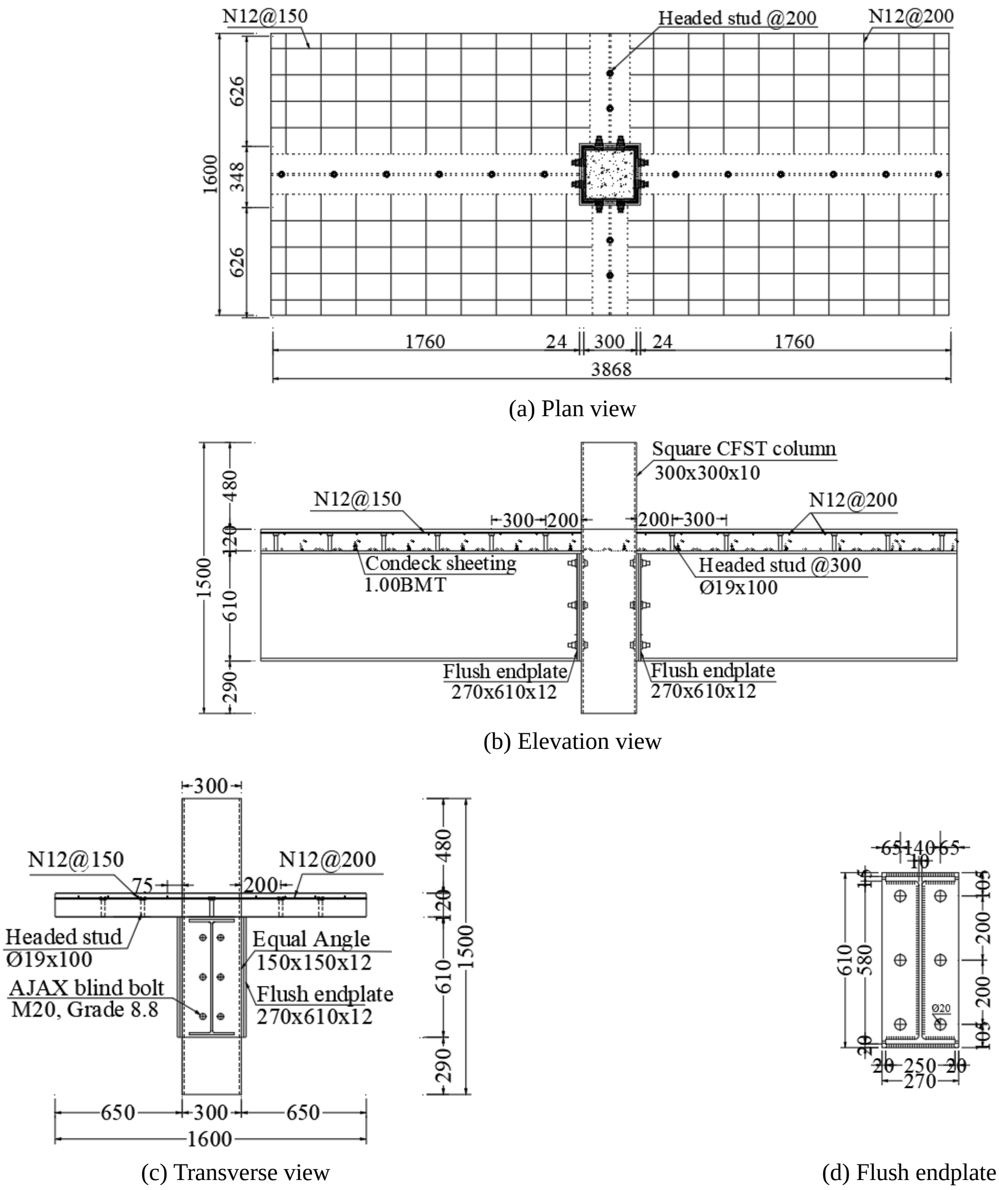

Fig. 1 Design moment-rotation characteristics of a joint (EN 1993-1-8 2010)

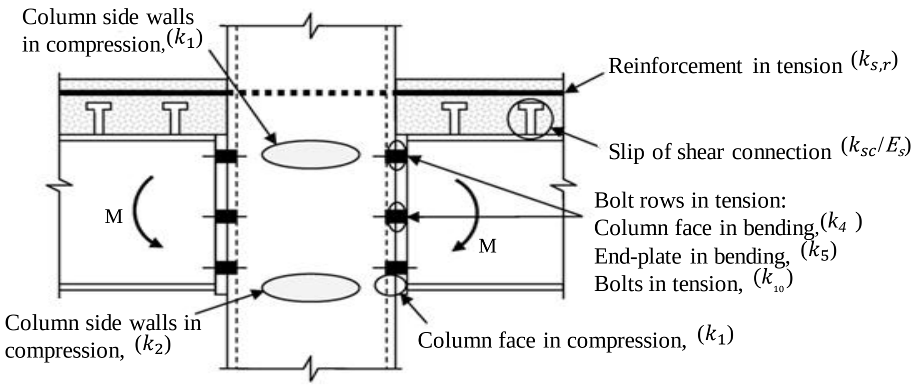

Fig. 2 Identification of components of the composite joint (Thai and Uy 2016)

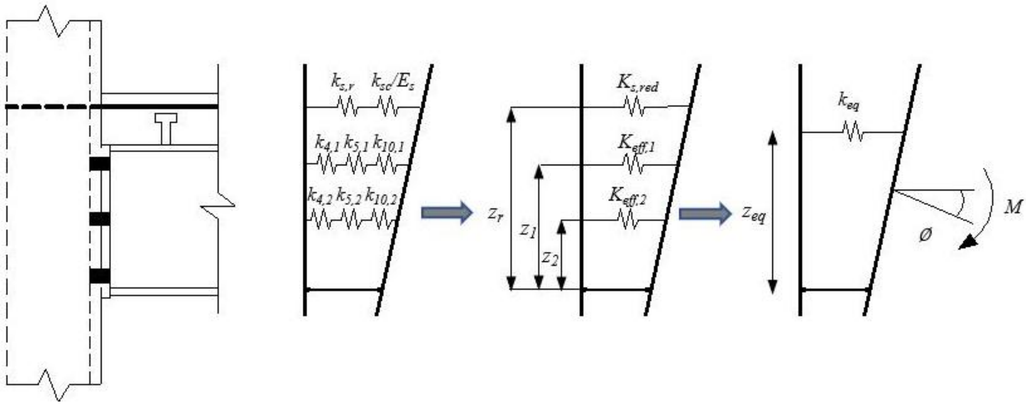

Fig. 3 Spring model for joints with CFST columns (Thai and Uy 2016)

$$S_{ini} = \frac{Ez_{eq}^2}{\frac{1}{k_{eq}}} \tag{2}$$

3.2 Prediction of design moment resistance, *Mj*, *Rd*

For a beam-to-column joint with a bolted end-plate connection, the design moment resistance can be calculated in accordance with EN 1993-1-8 as follows

$$M_{j,Rd} = \sum h_r F_{tr,Rd} \tag{3}$$

where, $F_{tr,Rd}$ is the effective design tension resistance of the bolt row r in consideration, hr is the distance from bolt row to the centre of compression and r is the number of bolt row. EN 1993-1-8 states that the effective design tension resistance $F_{tr,Rd}$ of a bolt row should be selected as the lowest value of the design tension resistance for an individual bolt row of the following components

1. Column web in tension, $F_{t,wc,Rd}$
2. Column flange in bending, $F_{t,fc,Rd}$
3. Reinforcement in tension, $F_{t,r,Rd}$
4. Endplate in bending, $F_{t,ep,Rd}$
5. Beam web in tension, $F_{t,wb,Rd}$

Each of these components can be calculated in accordance with the procedure presented in EN 1993-1-8.

3.3 Moment-rotation model

A design moment-rotation curve should represent three major structural properties which are moment resistance, initial stiffness and rotation capacity. EN 1993-1-8 describes a joint in terms of a rotational spring that connects the centre line of all the connecting members at a point of intersection as presented in Fig. 4.

The moment-rotation curve can be broadly classified according to three major stages. The first stage is the elastic stage and its slope is equal to the initial stiffness of the joint that is presented in Eq. (4). The second stage is the inelastic stage and the third stage relates to the strain hardening behaviour. The moment capacity was predicted using two different models as discussed by Wang *et al*. (2018a). The method adopted follows the guidelines from EN 1993-1-8 to predict the moment-rotation behaviour in the elastic stage whereas the model developed by Yee and Melchers (1986) was used for the inelastic and strain hardening stage. The slope of the inelastic stage can be determined as follows

$$S_j = \frac{Ez^2}{\mu \sum_i \frac{1}{k_i}} \tag{4}$$

where, k_i is the stiffness coefficient for basic joint component, z is the lever arm, μ is the stiffness ratio, $S_{j,\,ini}$ / S_j and its value is considered as 1 for the calculation of initial stiffness. According to EN 1993-1-8 two thirds of the

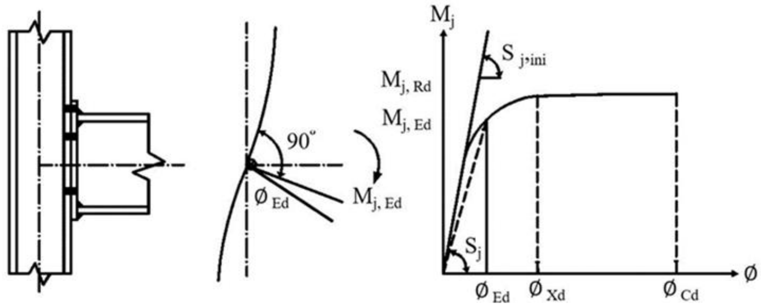

Fig. 4 Design moment-rotation characteristics of a joint (EN 1993-1-8 2010)

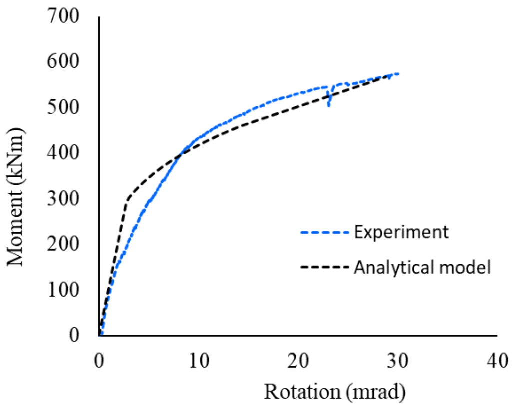

Fig. 5 Moment-rotation model

moment capacity define the maximum limit for the elastic stage. After that the initial stiffness will be reduced by the factor μ defined as

$$\mu = \left(\frac{1.5 M_{j,Ed}}{M_{j,Rd}} \right)^{\Psi} \tag{5}$$

3.4 Verification of the analytical model

The analytical models developed using the methods explained in Sections 3.1 and 3.2 were compared with the test results of Waqas *et al*. (2019) as shown in Fig. 5. It was observed that the modified moment-rotation model presented by Wang *et al*. (2018a) increased the accuracy of the predicted moment-rotation model as it agreed with the test results better than if the moment-rotation curve from EN 1993-1-8 alone was used. In general, the predicted curve coincided with the test results quite closely. Further comparison of the analytical model have been made with the test results of specimen CJ-1 and CJ-2 tested by Loh *et al*. (2006a) which are summarized in Table 1. Overall, it can be concluded that the analytical models proved to be very accurate and reliable for the estimation of initial stiffness and moment capacity of the tested joints.

The moment capacity calculated using the method outlined in EN 1993-1-8 and EN 1994-1-1 as discussed in Section 3.2 is based on the yielding of joint components which is lesser than the ultimate moment resistance. It is due to the fact that the yielding of components does not usually result in failure of the structure. The analytical models were used to investigate the performance of the composite frames under various types of design loads. The structural components of the frame did not achieve failure under the action of these design loads. Therefore, it is appropriate to use the analytical models in the analysis of the composite frame.

4. Conversion of composite section to equivalent steel section

4.1 Composite beams

EN 1994-1-1 defines the length of hogging moment region to span 15% to 25% of the beam length on each side of the internal support. This value was selected as $0.15L_b$ in this study. The composite section cannot be directly defined in Abaqus software (Abaqus 2014), therefore it was converted to an equivalent steel section that had the same stiffness and cross-sectional properties using modular ratio, α_m.

$$\alpha_m = \frac{E_s}{E_c} \tag{6}$$

The effective width of the composite slab at hogging

Table 1 Validation between analytical results and test results

Specimen		Moment resistance (kNm)			Initial stiffness (kNm/mrad)		
		Test	Predicted	Predicted/Test	Test	Predicted	Predicted/Test
Waqas *et al*. 2019	S-1	591.3	584.9	0.99	99.74	95.1	0.95
	S-2	601.6	584.9	0.97	99.25	95.1	0.96
Loh *et al*. 2006a	CJ-1	185.80	180.6	0.97	40	39..3	0.98
	CJ-2	187.95	181.4	0.96	38	33.7	0.88

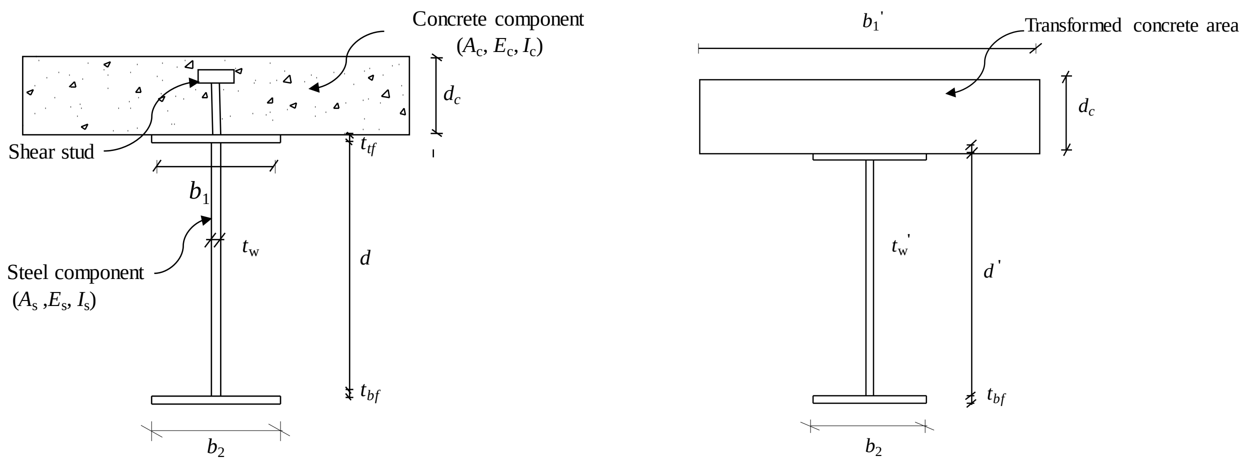

(a) Original section (b) Converted cross-section

Fig. 6 Cross-section conversion of composite beam to steel beam

Table 2 Details of the converted cross-section of composite beam to steel beam

Section	Details
Hogging moment region	b_3 = 290 mm, d_c = 120 mm b_2 = 228 mm, t_{fb} = 14.8 mm d' = 587.2 mm, t_w = 9.9 mm
Sagging moment region	b_3 = 350 mm, d_c = 120 mm b_2 = 228 mm, t_{fb} = 14.8 mm d' = 587.2 mm, t_w = 10.1 mm

and sagging moment region was calculated separately, based on the guidelines of EN 1994-1-1 as follows

$$b_{eff} = b_0 + \frac{0.5L_b}{8} + \frac{0.5L_b}{8} \quad (7)$$

$$b_{eff} = b_0 + \frac{0.7L_b}{8} + \frac{0.7L_b}{8} \quad (8)$$

The effective width of concrete slab at hogging moments was 1,125 mm whereas for sagging moment region it was 1,575 mm. Moreover, EN 1998-1 (2004) suggested a different method to calculate the effective width when considering seismic actions on the frames. According to that the effective width of concrete slab was calculated as 1,800 mm for hogging and 1,350 mm for sagging region. The cross-section area of concrete slab for sagging and hogging moment regions was calculated according to EN 1994-1-1 which was used to calculate the transformed cross-section area of the composite beam individually for both regions as follows

$$A_0 = A_s + \frac{A_{ce}}{\alpha_m} \quad (9)$$

After that, the location of neutral axis and second moment of area of the converted composite beam for both regions was calculated. Fig. 6 illustrates the conversion of composite beam to steel beam and details of the converted cross-section are presented in Table 2.

4.2 Composite columns

According to EN 1994-1-1, the effective flexural stiffness of the composite column can be predicted by

$$(EI)_{eff} = k_0(E_s I_s + E_{s,r} I_{s,r} + k_e E_{cm} I_c) \quad (10)$$

where the correction factor k_0 is 0.5 and the calibration factor k_e is 0.9.

Since there was no reinforcement present inside the CFST column, so its effect can be ignored. Eq. (10) can be rewritten as

$$(EI)_{eff} = k_0(E_s I_s + k_e E_{cm} I_c) \quad (11)$$

4.3 Semi-rigid joints

In order to meet the drift limit requirements, it is necessary to adjust the stiffness of all components so that an optimal distribution of resistance to the drift can be achieved. Theoretically, the flexural stiffness of the semi-rigid connection lies between the two extremes defined by EN 1993-1-8 as rigid and pinned.

Among the advanced analysis techniques, the plastic hinge method is the most effective method of modelling beam-to-column semi-rigid joints. This element is superior to the conventionally used spring element and is also proposed by Liew *et al.* (2000) and Thai *et al.* (2016). Therefore, the semi-rigid connections were modelled as a connector element type named as hinge in which the translations were restricted while the flexural rotation was allowed only.

5. Calculation of design loads and load combinations

The loads acting on the frame were dead loads, live loads, wind loads and earthquake loads which were calculated in accordance with AS1170.0 (2002). Dead loads

Table 3 Loads acting on the composite frames

Storey	Dead load (kN/m)	Live load (kN/m)	Wind actions (kN)		Earthquake actions (kN)
			Windward	Leeward	
Earthquake actions (kN) First storey	19	13.5	52.65	28.44	24.9
Second storey	19	13.5	52.65	28.44	49.8
Third storey	10.3	0	26.28	14.22	41.9

Table 4 Details of various load combinations

Number	Strength limit state	Number	Serviceability limit state
LC1	$1.35G$	LC6	W
LC2	$1.2G+1.5Q$	LC7	$G+0.4Q+W$
LC3	$0.9G+W$	LC8	$G+0.7Q$
LC4	$1.2G+0.4Q+W$	LC9	F_{eq}
LC5	$G+0.3Q+F_{eq}$	LC10	$G+0.4Q$

consisted of the self-weight of the structural components such as concrete slab, steel beam, ceiling, services, partitions etc. Live load of 3 kPa was considered for an office building. The actual values of loads acting on the frame are presented in Table 3 whereas the details of load combinations are presented in Table 4.

For wind loads, the critical design wind speed of 50-year design working life and 1/1000 years annual probability of exceedance was selected in the analysis. The assumptions made for load calculations represented the maximum probable values critical to the frame. Wind pressure was calculated that considered the combined effects of external and internal wind pressure acting on the frame and windward and leeward wall pressures were determined. These pressures were then converted to equivalent point loads acting on each of the floor as shown in Fig. 10.

Similarly, the earthquake actions were determined using AS/NZS 1170.4 (2007) based on a 50-year design period and 1/2500 annual probability of exceedance. The total horizontal base shear was calculated initially which was later distributed as point loads with proportional increments to each floor. The calculated earthquake design loads acting on each storey of the frame are presented in Table 3.

6. Frame analysis

6.1 General description

The frame models were constructed with three main components including the converted columns, converted beams and semi-rigid connections. In the beginning, the selected column cross section was 400 × 400 × 8 mm with Grade 350. The beam section used was 460UB82.1 with Grade 350 while the thickness of concrete slab was 120 mm with compressive strength of 40 MPa. A two-dimensional analysis was performed to develop a preliminary investigation and general understanding on the behaviour of low to medium rise semi-continuous frames exposed to lateral loads of critical wind and moderate earthquake conditions in Australia.

Figs. 7 and 8 presents the elevation and plan view of a 3 bay by 3 storey frame model of a prototype building designated as an office building that is presented as the main case study herein. The floor plan of the building was 27 m × 27 m with three bays of 9 m length in each direction. The building consisted of three storeys with each being 4 m in height. The general details of the composite frame are presented in Table 5. The longer bay span makes it more demonstrative of the Australian building practice.

Even though the number of bays was kept same in both directions, the presence of continuous floor slab and secondary beams was a reason for higher stiffness of one in-plane direction as compared to the other. Torsional behaviour or any out-of-plane effects can be considered to

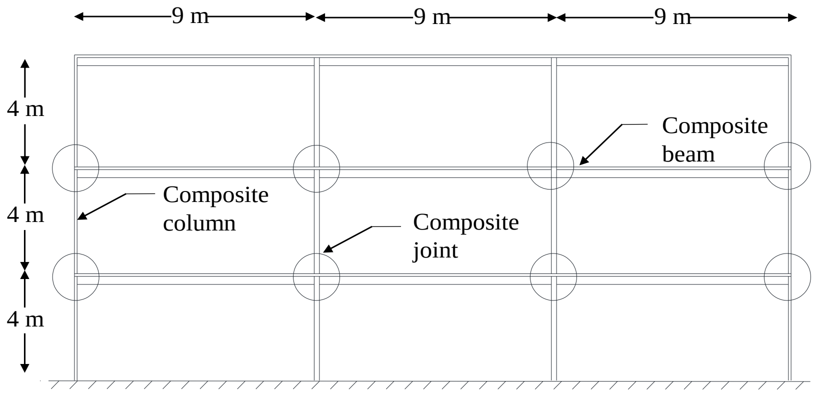

Fig. 7 Elevation of a typical 3 bay by 3 storey composite frame

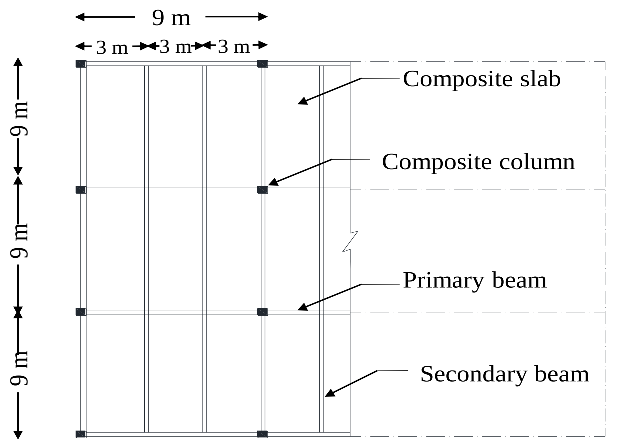

Fig. 8 Plan of a typical 3 bay by 3 storey composite frame

Table 5 General information on the design of frames

Feature	Range/Size
Number of storeys	2 - 5
Number of bays	2 - 4
Bay width	9 m × 9 m
Storey height	4 m

be insignificant. Hence the analysis can be simplified as a two-dimensional analysis considering in-plane direction.

6.2 Basic analysis procedure

A flowchart of the frame analysis procedure is presented in Fig. 9. It can be broadly divided into three stages. Stage 1 comprised of different calculations that were pre-requisite for the analysis. It consisted of the calculations of design loads and load combinations according to the Australian Standards AS1170.0 (2002), AS/NZS 1170.2 (2011) and AS/NZS 1170.4 (2007). Initial stiffness and moment capacity of the joint were calculated and moment-rotation models were developed. The composite beam and composite column were converted to an equivalent section of steel beam and steel column that were representative of similar cross-sectional properties as their composite counterpart. In second stage, the frame models were developed in Abaqus considering all geometrical and material nonlinearities. All the information calculated in Stage 1 was input into the software and the analysis was performed. The final stage involved interpretation of the results generated from the analysis and inspecting them against the limit state criteria from the Australian standards.

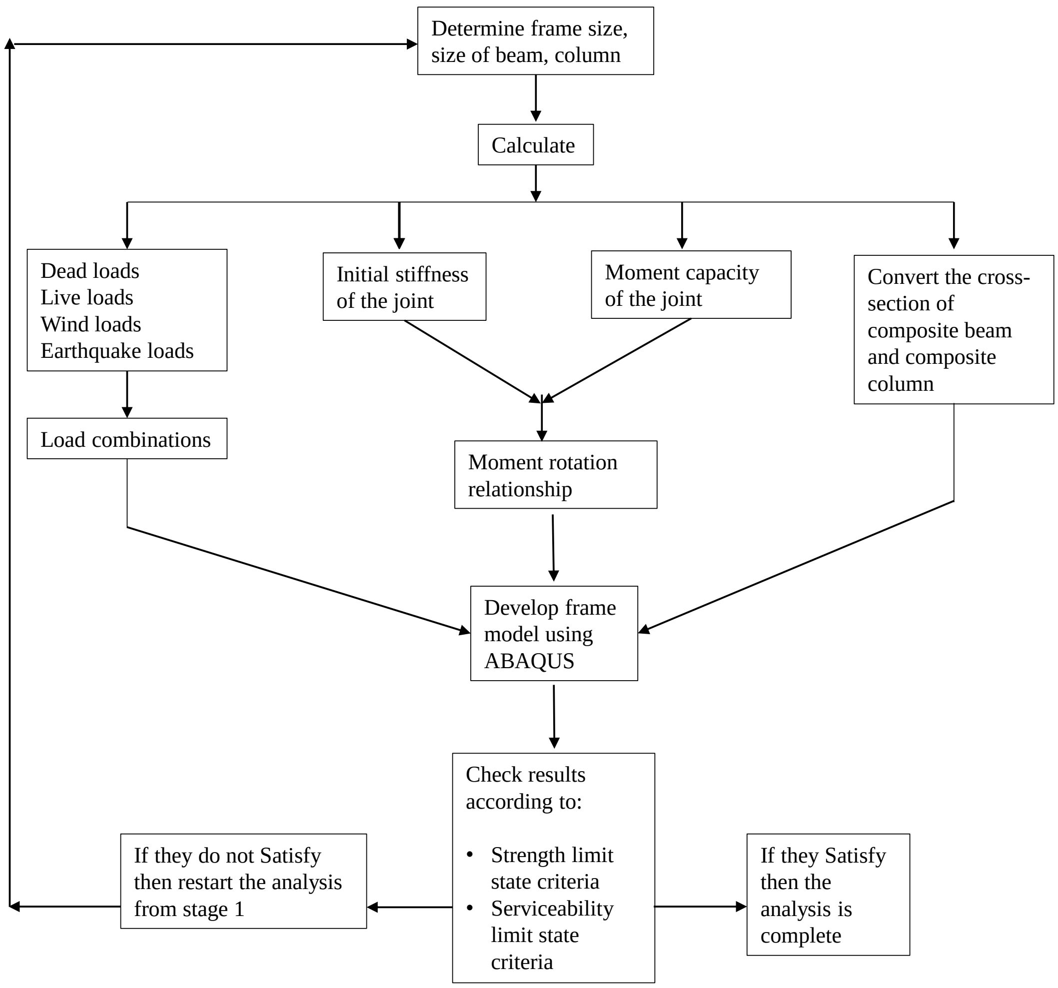

Fig. 9 Frame analysis procedure

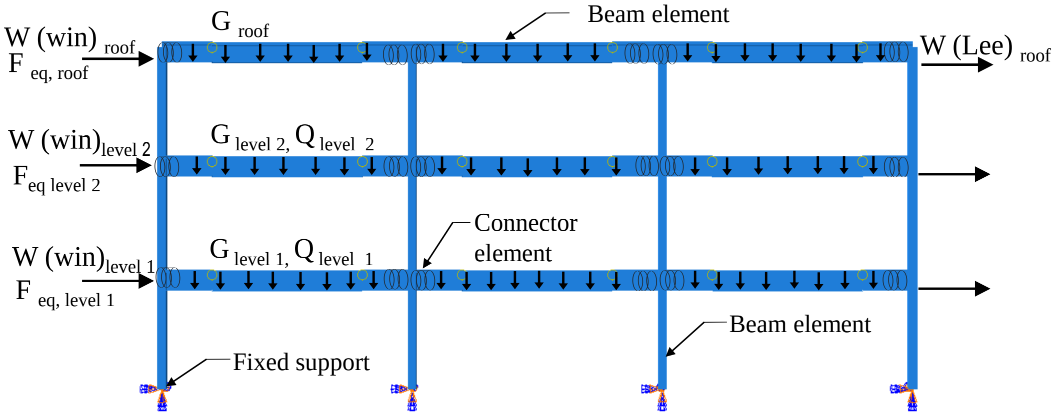

Fig. 10 A 3 bay by 3 storey composite frame in Abaqus software

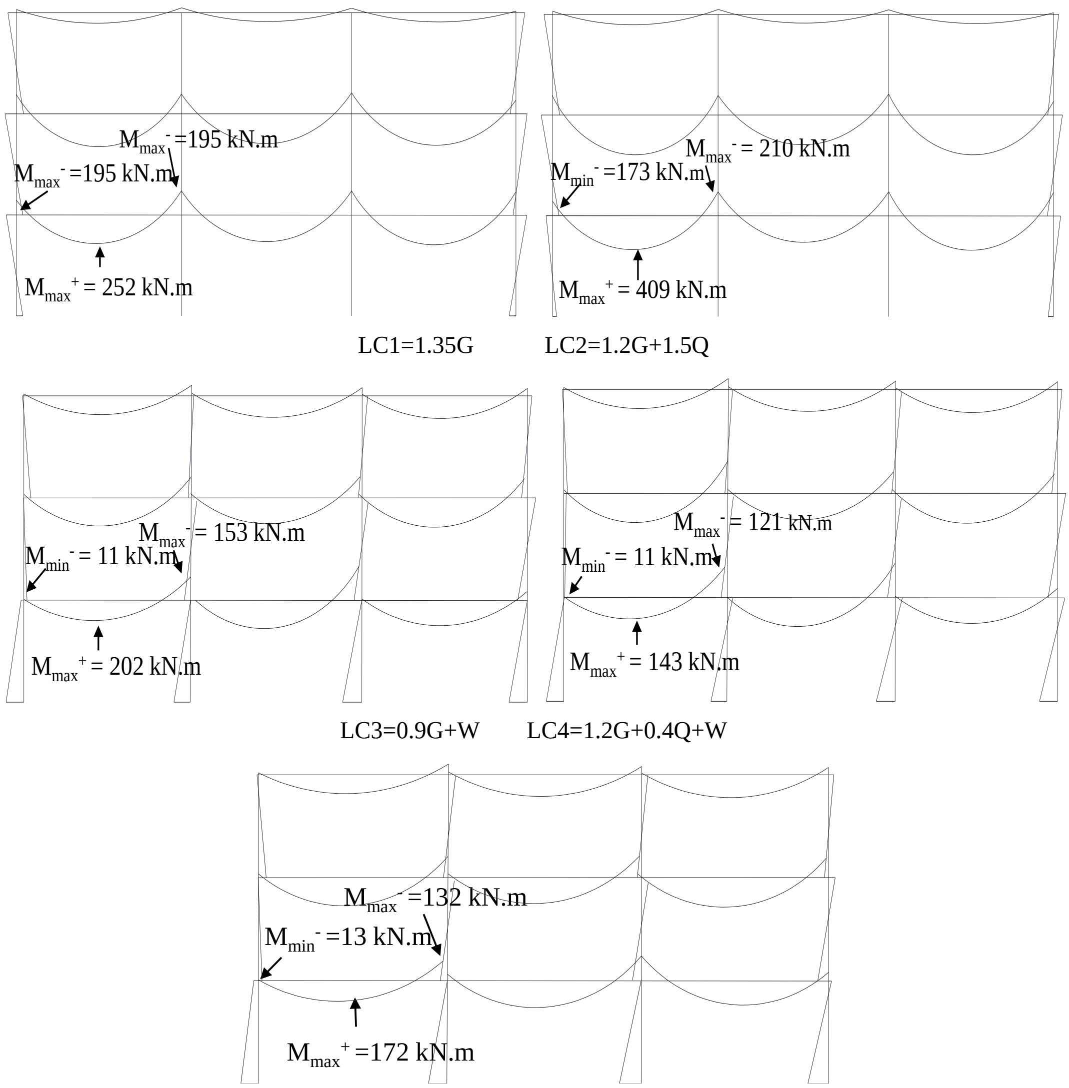

Fig. 11 Bending moment diagrams for 3bay by 3 storey frames in strength limit state

The design and analysis of the components ran in parallel as the moment distribution was affected by the stiffness and second moment of area. Hence, the component sizes were assumed at the beginning of the analysis. The results were checked against the design provisions specified in Australian standards and Eurocodes. If the results satisfied the requirements, they were accepted otherwise the frame was redesigned until the criteria were met. The analysis process involved hit and trial and was repeated unless a frame configuration was achieved that satisfied the limit states and did not involve overestimation of the member sizes. These criteria were as follows:

- AS/NZS 1170 suggested the mid span deflection limit of composite beams as L_b/250, where L_b represents the length of the beam
- In order to satisfy the serviceability requirement for an unbraced frame, a limit is imposed on the storey drift which is known as the horizontal displacement of a floor comparative to the floor underneath. AS1170.4 has enforced that limit on the inter-storey drift to be 1.5% for earthquake loading. In case of wind loading, this limit is specified as h_s/150, where hs represents the storey height
- The EN 1993-1-1 has proposed a more meticulous limit as h_s/300 in case of wind loading on the structures

6.3 Development of the frame models in Abaqus

6.3.1 General description

Abaqus software was used to accurately simulate the behaviour of all frames. The three main components of the frame that were precisely modelled included columns, beams and semi rigid connections. In addition to these, the proper selection of element type, adequate mesh size, load application and boundary conditions were the other significant parameters that were important to achieve accurate analysis results. A typical arrangement of a 3 bay by 3 storey frames in Abaqus is presented in Fig. 10.

6.3.2 Finite element type and mesh

Different element types were tried in order to find out the most suitable one to simulate the behaviour of the frame. From the Abaqus material library, beam element B31 was selected to model beams and columns. These are one-dimensional line elements in three-dimensional space that have stiffness affiliated with the deformation of the beam's axis. These elements were selected because they were preferred in global analysis models due to their computational efficiency. These elements were far more computationally efficient as compared with the solid elements since they had lesser degrees of freedoms. Hence, the speed of numerical simulation was increased. A comparison of numerical results between beam element models and solid element models was made to validate the reliability of finite element models using beam elements. The outputs including cross-section stress and vertical displacement were summarised in Table 6 and the moment-rotation curves of joints were displayed in Fig. 12. It is demonstrated that both results coincided with each other very well, indicating that the models with beam elements are capable to provide reliable prediction for frame analysis. It would be worth noting that no local buckling of beams was observed in the test specimens. Also, the beams used in the frame analysis were fully compacted. This further verifies the accuracy of the finite element model developed using beam elements.

Mesh convergence studies were conducted in order to find the most reasonable mesh that provided the most accurate results and also took lesser computational time.

Table 6 Comparison between beam and solid elements

		Beam element	Solid element	Beam/Solid
Cross-section normal stress (MPa)	Maximum	363.1	362	1.00
	Minimum	-157.6	-184.3	0.86
Cross-section normal stress (MPa)		350	350	1.00
Vertical displacement (mm)		94.7	94.1	1.01

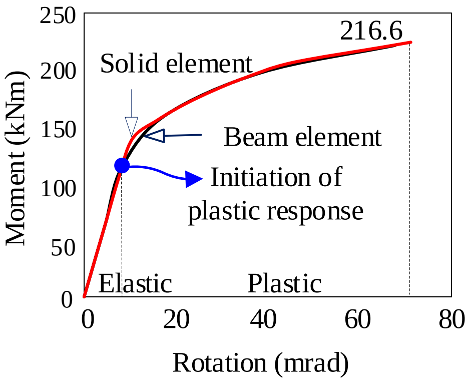

Fig. 12 Moment-rotation relationship of semi-rigid joint (Load combination 2)

Based on these results, it was found that accurate results can be achieved when an approximate global size of 125 mm length of global seeds was used for both beams and columns. The finite element mesh of each beam contained approximately 74 nodes.

6.3.3 Loading and boundary conditions

The bottom surfaces of all concrete filled steel tubular columns were fixed against all degrees of freedoms. This assumption of rigid base was also made by Hensman and Nethercot (2002), Yao *et al*. (2009) and Wang *et al*. (2018a). Although such degree of flexibility of a column base is hard to achieve in real practice as majority of the footings are not perfectly rigid in nature, this degree of flexibility becomes insignificant if the base connections are designed efficiently.

6.3.4 Material properties

The elastic-plastic material behaviour in Abaqus permits a multi-linear or bi-linear stress-strain curve to be used in the plastic option. This option was used to model the steel beam and steel column using a tri-linear elastic-plastic model. The first part of the tri-linear curve represents the elastic part up to the proportional limit followed by further yielding and strain hardening before fracture. The modulus of elasticity E was 200,000 N/mm^2 and poisson's ratio was 0.3. The yield stress of steel material was taken as 350 N/mm^2 and ultimate stress was 440 N/mm^2 corresponding to a plastic strain of 0.1819. However, the cross-section conversion of composite beams and columns was based on the equivalence of stiffness that incorporated elastic material behaviour. Hence, the beams and columns remained in the elastic range.

For semi rigid joints, the material behaviour was input in the connector sections in the form of moment-rotation models in order to include plastic behaviour. Two sets of the moment-rotation relationship data were assigned to the connector element with one representing hogging moment while the other representing sagging moment relationship. The moment-rotation model was input in ABAQUS using the "connector section" option. Details regarding connector element type and further details can be updated under this option. The connector type was selected as a "hinge" element which combines the connection types "JOIN" and "REVOLUTE" that allows rotational degrees of freedom but restrains translations. Furthermore, elasticity was input as non-linear in the behaviour options. Finally, the moment and rotation data calculated from the analytical model can be input in this section.

6.3.5 Analysis technique

Newton Raphson method was used in this study for analyzing the frame which is a very commonly used incremental solution technique. It is used to solve non-linear equilibrium equations and is a potentially good tool to capture non-linear behaviour of the structures.

7. Analysis results and discussions

Fig. 11 presents the bending moment diagrams for the 3 bay by 3 storey frame model that highlights the sagging and hogging bending moments under the load combinations in strength limit states.

The selected column cross section was 300 × 300 × 10 mm with Grade 350. The beam selected was 610UB101 with Grade 350 while the thickness of concrete slab was 120 mm. The general details of these components are presented in Table 7. It was observed that the load combination 2 incorporating gravity loads alone were most critical to frame in terms of producing maximum hogging moment as well as sagging bending moment. Load combinations 3 and 4 that represented the wind loading in Australia were observed to be more critical as compared to

Table 7 General information of the frame components

Specimen	Dimensional details
Steel column	300 × 300 × 10 mm, Grade 350, h_c = 4000 mm, t_c = 10 mm
Steel beam	610UB101 (602 × 228 ×14.8 × 10.6), Grade 350, d = 602 mm, b_b = 228 mm, t_w = 10.6 mm, t_f = 14.8 mm, A_b = 13000 mm^2, E_b = 2×10^5 Nmm^2, I_b = 761 × 10^6 mm^4
Concrete slab	d = 120 mm, b_{eff} = 626 mm, A_c = 75120 mm^2 f_c = 40 MPa, E_c = 32,800 MPa

Table 8 Maximum and minimum hogging bending moments for all frames in strength limit states

	Hogging bending moment (kN·m)		
	2 bays	3 bays	4 bays
2 storeys	255(33)	249(3)	250(31)
3 storeys	253(3)	240(11)	245(31)
4 storeys	210(26)	235(5)	243(26)
5 storeys	203(27)	249(3)	248(3)

*Note: The values inside brackets represents minimum and values outside brackets represents maximum hogging bending moments

Table 9 Maximum and minimum Sagging bending moments for all frames in strength limit states

	Sagging bending moment (kN·m)		
	2 bays	3 bays	4 bays
2 storeys	399(91)	409(91)	402(97)
3 storeys	391(89)	409(89)	400(95)
4 storeys	387(87)	407(89)	399(95)
5 storeys	383(83)	407(87)	397(91)

* Note: The values inside brackets represents minimum and values outside brackets represents maximum sagging bending moments

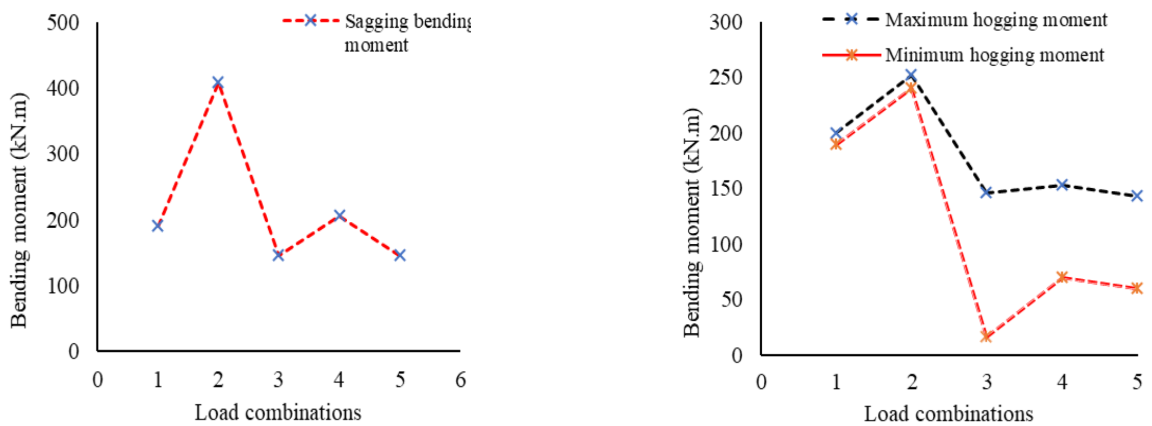

(a) Sagging bending moment (b) Hogging bending moment

Fig. 13 Variation of sagging and hogging bending moments for different load combinations in strength limit states load combination 5 that represented earthquake loading in Australia.

The serviceability behaviour of the frame was also found to be reasonable. The maximum drift for each storey was found to be 23 mm for the top most storey, 18 mm for the middle storey and 11 mm for the following storey. It was also found that the sway displacement on the ground floor was the most critical. Limiting the drift of this floor would respond in a satisfactory drift for all other floors too. The maximum long-term beam deflection due to creep and shrinkage was found to be satisfactory as well.

The results of maximum and minimum hogging and sagging bending moments are presented in Tables 8 and 9. The maximum hogging moments occurred under the effect of load combination 2. Therefore, the moment-rotation relationship of the semi-rigid joint was extracted from Abaqus for LC2 which is presented in Fig. 12. It can be observed that the bolted flush endplate joints experienced plastic behaviour. The maximum value of hogging moment was found to be 216.6 kN.m. The variation of sagging and hogging bending moments for different load combinations in strength limit states is presented in Fig. 13.

For the total range of frames, it was observed that the moment reversal did not occur at any of the interior supports when lateral loads of wind or earthquake were applied except for the tall and slender frames with 2 bay by by 5 storey and 2 bay by 4 storey size. It was also observed that the maximum values of hogging and sagging moments always appeared in the exterior span on the ground floor.

8. Conclusions

A range of moment resisting composite frames has been designed and analysed in accordance with Australian standards and Eurocodes. Details of all necessary calculations have been presented following up with the development and analysis of the frame model using Abaqus. Within the present scope of investigation, the following conclusions can be made.

- Comparison of the predicted initial stiffness and moment capacity with the test results demonstrates that the moment-rotation model is accurate and reliable to be adopted for further application;
- The structure performs adequately when it is subjected to the applied gravity and lateral loads of wind and earthquake. Load combination incorporating gravity loads governs the design for all cases except for 2 × 5 and 2 × 4 storey frames. Among lateral loads, wind loads are more critical as compared to the earthquake loads in Australia;
- For low to medium rise buildings, the design of ground floor is critical to the drift limit. No moment reversal occurred except for 2 bay by 5storey and 2 bay by 4 storey frames. Hence, it is suggested that tall and slender frame designs should be avoided. More number of bays would be advantageous in this case;
- The results from the analysis are helpful for understanding the complicated behaviour of blind bolted composite frames and can be applied to the design of these types of frames in engineering practice.

Acknowledgments

The research work presented in this paper was financially supported by the Australian Research Council (ARC) Linkage grants (LP110200511) programme with their industry partners Ajax Engineered Fasteners and Orrcon Steel. The authors would like to express gratitude to the funding sponsors for their support.

References

Abaqus (2014), User Manual; Version 6.14, DS SIMULIA Corp., Providence, RI, USA.

Abolmaali, A., Matthys, J.H., Farooqi, M. and Choi, Y. (2005), "Development of moment-rotation model equations for flush end-plate connections", *J. Constr. Steel Res.*, **61**(12), 1595-1612.

Ahmed, B. and Nethercot, D.A. (1997), "Prediction of initial stiffness and available rotation capacity of major axis composite flush endplate connections", *J. Constr. Steel Res.*, **41**(1), 31-60.

AISC-LRFD (1994), Manual of steel construction, load and resistance factor design, (2nd Ed.).

AS/NZS 1170.0-2002 (2002), Structural design actions. part 0: general principles; Australia.

AS/NZS 1170.1-2002 (2002), Structural design actions. part 1: permanent, imposed and other actions; Australia.

AS/NZS 1170.2-2011 (2011), Structural design actions. part 2: wind actions; Australia.

AS/NZS 1170.4-2007 (2007), Structural design actions. Part 4: Earthquake actions in Australia; Australia.

Beena, K., Naveen, K. and Shruti, S. (2017), "Behaviour of bolted connections in concrete-filled steel tubular beam-column joints", *Steel Compos. Struct., Int. J.*, **25**(4), 443-456.

EN 1993-1-1 (2005), Eurocode 3: Design of steel structures. part 1–1: general rules and rules for buildings; European Committee for Standardization, Brussels, Belgium.

EN 1993-1-8 (2010), Eurocode 3: Design of steel structures. part 1–8: design of joints; European Committee for Standardization, Brussels, Belgium.

EN 1994-1-1 (2004), Eurocode 4: Design of composite steel and concrete structures. part 1–1: general rules and rules for buildings; European Committee for Standardization, Brussels, Belgium.

EN 1998-1 (2004), Eurocode 8: Design of structures for earthquake resistance. part 1: general rules, seismic actions and rules for buildings; European Committee for Standardization, Brussels, Belgium.

Ghobarah, A., Mourad, S. and Korol, R.M. (1996), "Moment-rotation relationship of blind bolted connections for HSS columns", *J. Constr. Steel Res.*, **40**(1), 63-91.

Gomes, F., Jaspart, J.P. and Maquoi, R. (1994), "Behaviour of minor-axis joints and 3D joints", *Proceedings of the Second State of the Art COST C1 Workshop on Semi Rigid Connections*, Prague, Czech Republic, pp. 111-120.

Gomes, F., Jaspart, J.P. and Maquoi, R. (1996), "Moment capacity of beam-to-column minor-axis joints, *Proceedings of the Second State of the IABSE Colloquium on Semi-rigid Structural Connections*, pp. 319-326.

Han, L.H., Wang, W.D. and Zhao, X.L. (2008), "Behaviour of steel beam to concrete-filled SHS column frames: Finite

element model and verifications", *Eng. Struct.*, **30**(6), 1647-1658.
Han, C., Li, Q., Wang, X., Jiang, W. and Li, W. (2016), "Research on rotation capacity of the new precast concrete assemble beam-column joints", *Steel Compos. Struct., Int. J.*, **22**(3), 613-625.
Hensman, J.S. and Nethercot, D.A. (2001), "Numerical study of unbraced composite frames: generation of data to validate use of the wind moment method of design", *J. Constr. Steel Res.*, **57**, 791-809.
Jeyarajan, S. and Liew, J.R. (2016), "Robustness analysis of 3D Composite buildings with semi-rigid joints and floor slab", *Structures*, **6**, 20-29.
Lee, S.S. and Moon, T.S. (2002), "Moment-rotation model of semi rigid connections with angles", *Eng. Struct.*, **24**, 227-237.
Liew, J.R., Teo, T.H., Shanmugam, N.E. and Yu, C.H. (2000), "Testing of steel -concrete composite connections and appraisal of results", *J. Constr. Steel Res.*, **56**(2), 117-150.
Loh, H.Y., Uy, B. and Bradford, M.A. (2006a), "The effects of partial shear connection in composite flush end plate joints - Part I – Experimental study", J. Constr. Steel Res., 62(4), 378-390.
Loh, H.Y., Uy, B. and Bradford, M.A. (2006b), "The effects of partial shear connection in composite flush end plate joints - Part II - Analytical study and design appraisal", *J. Constr. Steel Res.*, **62**(4), 391-412.
Li, D.X., Uy, B., Patel, V. and Aslani, F. (2017), "Analysis and design of demountable embedded steel column base connections", *Steel Compos. Struct., Int. J.*, **23**(3), 303-315.
Ma, H.W., Jiang, W.S. and Cho, C. (2011), "Experimental study on two types of new beam-to-column connections", *Steel Compos. Struct., Int. J.*, **11**(4), 291-305.
Nogueiro, P., Silva, L.S.D., Bento, R. and Simões, R. (2009), "Calibration of model parameters for the cyclic response of end-plate beam-to-column steel-concrete composite joints", *Steel Compos. Struct., Int. J.*, **9**(1), 39-58.
Thai, H.T. and Uy, B. (2015), "The application of Eurocode 4 to blind bolted endplate composite joint", *Proceedings of the 2015 World Congress on Advances in Structural Engineering and Mechanics* (*ASEM*), Incheon, Korea.
Thai, H.T. and Uy, B. (2016), "Rotational stiffness and moment resistance of bolted endplate joints with hollow or CFST columns", *J. Constr. Steel Res.*, **126**, 139-152.
Thai, H.T., Uy, B., Kang, W.H. and Hicks, S. (2016), "System reliability evaluation of steel frames with semi-rigid connections", *J. Constr. Steel Res.*, **121**, 29-39.
Uy, B. (2012), "Applications, behaviour and design of composite steel-concrete structures", *Adv. Struct. Eng.*, **15**(9), 1559-1571.
Uy, B., Patel, V., Li, D.X. and Aslani, F. (2017), "Behaviour and design of connections for demountable steel and composite structures", *Structures*, **9**, 1-12.
Wang, J., Uy, B. and Li, D. (2018a), "Analysis of demountable steel and composite frames with semi-rigid bolted joints", *Steel Compos. Struct., Int. J.*, **28**(3), 363-380.
Wang, J., Uy, B., Thai, H.T. and Li, D.X. (2018b), "Behaviour and design of demountable beam-to-column composite bolted joints with extended end-plates", *J. Constr. Steel Res.*, **144**, 221-235.
Waqas, R., Uy, B. and Thai, T. (2015), "Parametric studies on the behaviour of beam-column flush endplate connections using blind bolts", *Proceedings of the 2015 World Congress on Advances in Structural Engineering and Mechanics* (*ASEM*), Incheon, Korea.
Waqas, R., Uy, B. and Thai, T. (2019), "Experimental and numerical behaviour of blind bolted flush endplate composite connections", *J. Constr. Steel Res.*, **153**, 179-195
Xiao, Y., Choo, B.S. and Nethercot, D.A. (1996), "Composite connections in steel and concrete. Part 2- Moment capacity of end plate beam to column connections", *J. Constr. Steel Res.*, **37**, 63-90.
Yao, H., Goldsworthy, H. and Gad, E. (2009), "Design and analysis of a case study low-rise building with moment resisting composite frames", *Australian Earthquake Engineering Society Conference*, Newcastle, NSW, Australia.
Yee, Y.L. and Melchers, R.E. (1986), "Moment-Rotation Curves for Bolted Connections", *J. Struct. Eng.*, **112**(3), 615-635.
Zhao, H. (2016), "Analysis of seismic behavior of composite frame structures", *Steel Compos Struct., Int. J.*, **20**(3), 719-729.

DL

Notations

A_0	Converted cross-section area of composite beam
A_s	Cross-section area of steel
D	Depth of concrete slab
E_s	Modulus of elasticity of structural steel
E_{cm}	Modulus of elasticity of concrete
$E_{s,r}$	Modulus of elasticity of reinforcing steel
$(EI)_{eff}$	Effective flexural stiffness of composite columns
F_{eq}	Earthquake actions
G	Dead loads
h_c	Height of inter-storey columns
I_b	Second moment of inertia of beam's section
I_c	Second moment of area of infilled concrete core
I_s	Second moment of area of steel tube
K_0	Correction factor
K_e	Calibration factor
L_b	Span of beams between columns
$M_{j,Rd}$	Design moment resistance of beam-to-column joints
$M_{j,Ed}$	Bending moment of beam-to-column joints
N	Number of shear connectors
Q	Live loads
S_j	Stiffness of beam-to-column joints
$S_{j,ini}$	Initial stiffness of beam-to-column joints
W	Wind actions
b_{eff}	Effective width of the concrete slab
d_s	Distance between longitudinal reinforcing bars in tension and centroid of the steel beam's section
h	Distance between centroid of beam flanges in tension and centroid of beam flanges in compression
h_s	Distance between longitudinal reinforcing bars in tension and centroid of beam flanges in compression
k_B	Stiffness coefficient for blind bolts
k_c	Stiffness coefficient for column walls
k_{eff}	Effective stiffness coefficient
k_{ep}	Stiffness coefficient for end-plates
k_{eq}	Equivalent stiffness coefficient for beam-to-column joints
k_i	Stiffness coefficient for basic components
k_{sc}	Stiffness coefficient for shear connectors
k_{slip}	Reduction factor of stiffness coefficient
$k_{s,r}$	Stiffness coefficient for reinforcing bars
t_p	thickness of flush endplate
z_{eq}	Equivalent lever arm
v	Poisson's ratio
φ	Factor of initial stiffness
ϕ_j	Rotational deformations of beam-to-column joints